JOC The Journal of Organic Chemistry

Article

pubs.acs.org/joc

Ion Pair Recognition Receptor Based on an Unsymmetrically 1,1′-Disubstituted Ferrocene−Triazole Derivative

Francisco Otón,*[,†] María del Carmen González,[†] Arturo Espinosa,[†] Carmen Ramírez de Arellano,[‡] Alberto Tárraga,*[,†] and Pedro Molina*[,†]

[†]Departamento de Química Orgánica, Facultad de Química Campus de Espinardo, Universidad de Murcia, E-30100 Murcia, Spain

[‡]Departamento de Química Orgánica, Facultad de Farmacia, Universidad de Valencia, E-46100 Valencia, Spain

Supporting Information

ABSTRACT: The ferrocene−triazole derivative **4**, available from 1,1′-bis(diazido)ferrocene by sequential functionalization through click-type chemistry and the Staudinger reaction, is elaborated as a lab-on-a-molecule for the selective sensing of $HP_2O_7^{3-}$ and Hg^{2+}. Receptor **4** behaves as a ratiometric fluorescent probe for $HP_2O_7^{3-}$ with a good selectivity over other anions, whereas in the presence of Hg^{2+} it modifies the fluorescent emission of the pyrene unit, acting as a selective on−off fluorescent sensor for Hg^{2+} with a low detection limit. The most salient feature of compound **4** is its behavior as an excellent electrooptical ion pair recognition receptor able to simultaneously recognize Pb^{2+} cations in the presence of $HP_2O_7^{3-}$ anion through multichannel perturbations of the redox potential of the ferrocene unit, the emission spectrum, and a noticeable color change from yellow to green.

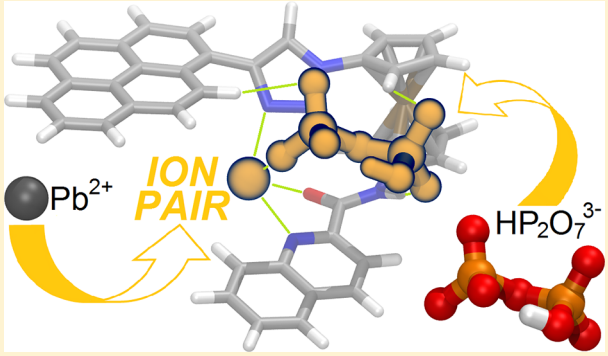

INTRODUCTION

The design and synthesis of heteroditopic receptors containing recognition sites for both cations and anions, that is, ion pair recognition receptors, is an emerging field in modern supramolecular chemistry.[1] In particular, the design of ion pair receptors that can respond to a discriminative stimulus is very engaging. Such systems are interesting not only as switches[2] but also in drug delivery[3] and molecular sensing[4] or as templates for inducing the formation of complex supramolecular structures.[5] The scope and relevance of this field of research is illustrated by the potential applications of ion pair receptors in membrane transport and their enhanced ability to solubilize otherwise insoluble ions, remarkable capacity to extract certain ion pairs from water, and selectivities for targeted ions that are superior to those of simple ion receptors. Despite these practical applications, the number of well-characterized ion pair receptors remains limited. Presumably, this reflects their synthetic difficulties, as well as experimental complexities resulting from the more elaborate nature of the binding phenomena involved.

Ferrocene−triazole derivatives are one of the systems that have potential applications in the field of electrochemical detection and sensing and host−guest chemistry.[6] The 1,2,3-triazole motif has proved to be a versatile ion recognition unit for both cations and anions. As nitrogen-containing Lewis bases, triazole-based ligands have been shown to coordinate transition-metal cations.[7] In contrast, several triazole derivatives recognize anions through a cooperative triazole C−H···anion hydrogen bond.[8] Hence, the integration of the triazole motif into the design of heteroditopic receptors for ion pair recognition is an attractive proposition. Surprisingly, to the best of our knowledge, only three examples of triazole-containing[9] and ferrocene-containing[10] ditopic receptors have been reported, whereas no example based on an unsymmetrically 1,1′-disubstituted ferrocene has been described.[11]

Unsymmetrically 1,1′-disubstituted ferrocene derivatives can lead to improved multifunctional systems for molecular recognition processes. Thus, in a monosubstituted ferrocene a different substituent at the other cyclopentadienyl ring can induce an intermolecular interaction or a change in the electrochemical parameters.[12] Importantly, known synthetic methodologies for the preparation of unsymmetrically 1,1′-disubstituted ferrocene derivatives involve complex transformations.[13] The methods of their preparation involve selective introduction of a second substituent in the 1′-position of a monosubstituted derivative or selective transformation of one substituent of symmetrically disubstituted compounds.

In this context, we report the synthesis, structural characterization, and sensing properties of an unusual ion pair recognition receptor bearing a central unsymmetrically 1,1′-disubstituted ferrocene. The presence of multiple binding sites in the designed new structural motif and the multiresponsive character of the receptor are most noteworthy, allowing its use as an electrooptical multisignaling ion pair recognition receptor. The central ferrocene unit is linked to a pyrene through a 1,2,3-

Received: July 30, 2012
Published: October 22, 2012

Scheme 1. Synthesis of Receptor 4[a]

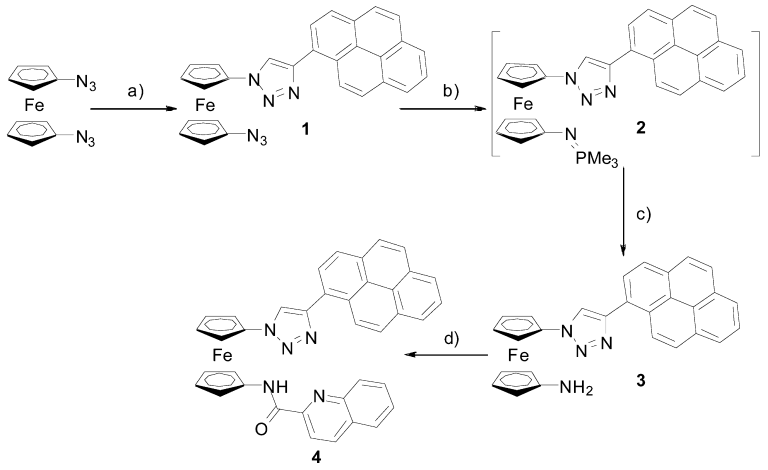

[a]Reagents and conditions: (a) ethynylpyrene, $CuSO_4$, sodium ascorbate, THF/water; (b) trimethylphosphine, anhydrous THF; (c) water; (d) 2-quinaldoyl chloride, anhydrous THF.

triazole at one cyclopentadienyl ring, whereas the other one is substituted by a quinoline heteroaromatic ring linked through an amide bridge. On these bases, suitable dual signaling chemical probes can be built by combining the redox activity of ferrocene,[14] the photoactivity of the pyrene,[15] and the proved binding ability of the 1,2,3-triazole ring,[8] the amide group,[16] and the quinolone ring.[17]

RESULTS AND DISCUSSION

Synthesis. The synthetic procedure followed for the preparation of compound **4** is summarized in Scheme 1. This methodology requires, as a key intermediate, compound **1**, which can be prepared starting from the 1,1′-bisazidoferrocene, previously synthesized in a two-step sequence: bislithiation of ferrocene and subsequent treatment with (2,4,6-triisopropylphenyl)sulfonyl azide (trisyl azide).[18] The conversion of 1,1-bisazidoferrocene into **1** was then achieved in a one-step process by monofunctionalization of one azide group of the starting material by using the click reaction[19] with the appropriate amounts of ethynylpyrene and a copper(II) sulfate/sodium ascorbate mixture. The intermediate compound **1** underwent a Staudinger reaction with trimethylphosphine under anhydrous conditions to give the highly reactive iminophosphorane derivative **2**, which could not be isolated. Subsequent hydrolysis provided the corresponding amine **3** in 64% yield. Finally, reaction of amine **3** with 2-quinaldoyl chloride provided the receptor **4** in 86% yield.

The structures of compounds **1**−**4** have been confirmed by the usual techniques (^{1}H NMR, ^{13}C NMR, FT-IR, MS, and elemental analysis). In addition, the structure of compound **4** was also confirmed by single-crystal X-ray diffraction (XRD) analysis (Figure 1). The compound **4** crystal structure shows a folded conformation with the pyrene and quinoline rings almost coplanar, with short distances that suggest a $\pi-\pi$ interaction (mean distance 3.5 Å). The amide group is coplanar with both the quinoline ring and the cyclopentadienyl ring directly attached. The amide group N−H bond (N1−H1) forms a short contact with the quinoline nitrogen atom (N11) (N1−H1···N11: H1···N11, 2.28(2) Å; N1···N11, 2.680(2) Å; N1−H1···N11, 111.9(18)°). The triazole unit is considerably out of the planes formed by the pyrene or the adjacent Cp ring (dihedral angles of 34.11° and 35.70°, respectively). In the

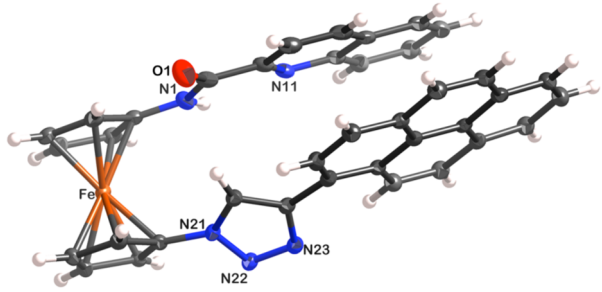

Figure 1. X-ray ellipsoid plot for compound **4** (50% probability level).

crystal, the molecules adopt a herringbone packing mode with the C−H, C═O, and N−H bonds of a molecule oriented toward the π cloud of the neighboring molecule. The conformation of the receptor **4** in the crystal structure, having substituents at the 1- and 1′-positions of the ferrocene moiety oriented to the same site, can be explained by taking into account that the rotational barrier of 1,1′-disubstituted ferrocenes should be easily overcome at room temperature.[20] Thus, the situation observed for receptor **4** should be a result of a compromise of steric repulsions and possible attractive forces between substituents. Among the latter, π,π-stacking between parallel aromatic planes in substituents in the 1- and 1′-positions is commonly reported in the literature.[7r]

Cation and Anion Binding Studies. Electrochemical and optoelectronic properties of receptor **4** have been studied as well as its binding properties toward cations (Li^+, Na^+, K^+, Mg^{2+}, Ca^{2+}, Ni^{2+}, Cu^{2+}, Zn^{2+}, Cd^{2+}, Hg^{2+}, and Pb^{2+}) and their perchlorate or triflate salts (Li^+, K^+, Mg^{2+}, Ni^{2+}, Cd^{2+}, and Pb^{2+} were added as perchlorate salts, while Na^+, Ca^{2+}, Cu^{2+}, Zn^{2+}, and Hg^{2+} were added as triflate salts) and anions (F^-, Cl^-, Br^-, AcO^-, NO_3^-, HSO_4^-, $H_2PO_4^-$, and $HP_2O_7^{3-}$ as TBA^+ salts).

The cyclic voltammogram of **4** ($c = 5 \times 10^{-4}$ M) carried out in $CH_3CN/CH_2Cl_2/H_2O$ (90:8:2) using tetrabutylammonium hydrogen sulfate (TBAHP) (c = 0.1 M) as the supporting electrolyte exhibits a reversible oxidation wave with a half-wave potential of $E_{1/2}$ = 120 mV versus the redox pair Fc^+/Fc. This potential is identical to the redox peak found in the Osteryoung square-wave voltammetry (OSWV) technique (see the Supporting Information). The criteria applied for reversibility

dx.doi.org/10.1021/jo301570u | J. Org. Chem. 2012, 77, 10083−10092

were a separation of 60 mV between cathodic and anodic peaks, a ratio of 1.0 ± 0.1 for the intensities of the cathodic and anodic currents I_c/I_a, and no shift of the half-wave potential with varying scan rates.

The UV–vis spectrum of **4**, obtained out in the same solvent, shows three absorption bands that appear at λ = 243, 285, and 357 nm and a small shoulder near 276 nm that is hardly visible in the spectrum. The band in the limit of the visible region masks all the bands attributable to the ferrocene unit (d–d and metal–ligand charge transfer (MLCT) bands) that should appear in this region of the spectrum. Regarding the emissive characteristics of the receptor, **4** is characterized by an intense monomer band (Φ_F = 0.053) when it is excited at λ_{exc} = 350 nm. This band is characterized by a small Stokes shift ($\Delta\lambda$ = 41 nm) and the presence of a vibronic fine structure (see the Supporting Information).

Previous to the study of ion pair recognition, we carried out a detailed characterization of the anion and cation affinities of the receptor. The anion recognition capability of **4** has been tested toward the above-mentioned anionic species. The changes in the properties of the receptor have been studied by electrochemical, absorption, fluorescence, and ^{1}H NMR techniques. Concerning the deprotonation/coordination dualism, the electrochemical data strongly support that the $HP_2O_7^{3-}$ anion induces formation of a hydrogen-bonded complex between the receptor **4** and $HP_2O_7^{3-}$ anion. When the aforementioned anions were added to an electrochemical solution of the receptor **4** ($c = 5 \times 10^{-4}$ M) in $CH_3CN/CH_2Cl_2/H_2O$ (90:8:2), only $HP_2O_7^{3-}$ anion induced a clear perturbation of the oxidation wave. Thus, the stepwise addition of such an anion promotes a clear cathodic shift of the free receptor's oxidation wave with a maximum perturbation obtained ($\Delta E_{1/2}$ = −110 mV) when up to 10 equiv of $HP_2O_7^{3-}$ is added. Only in recent years have alternative mechanisms for several types of anion–receptor interactions been developed.[21] A possible way to reveal the formation of hydrogen-bonded complexes under conditions of electrochemical titration is to suppress deprotonation by adding a small amount of acetic acid.[22] In preliminary experiments, we found that addition of up to 20 equiv of acetic acid did not affect either the cyclic voltammetry (CV) or the OSWV of receptor **4**. On one hand, titration with a strong base such as Bu_4NOH, which definitely leads to deprotonation of the neutral receptor, gave rise to the appearance of a new oxidation wave, cathodically shifted by a magnitude ($\Delta E_{1/2}$ = −180 mV) different from that obtained in the case of the $HP_2O_7^{3-}$ anion (see ESI). On the other hand, the results obtained upon titration with $HP_2O_7^{3-}$ in the presence of 20 equiv of AcOH, to avoid any deprotonation process, clearly showed a significant cathodic shift by −90 mV. These data indicate that the perturbations observed upon addition of this anion to the free receptor **4** should be associated with a recognition event, involving the formation of a hydrogen-bonded complex between receptor **4** and the $HP_2O_7^{3-}$ anions.

The recognition behavior of receptor **4** toward anions was also studied by UV–vis spectroscopy. When the set of anions was added to the solution of the receptor ($c = 2 \times 10^{-5}$ M) in $CH_3CN/CH_2Cl_2/H_2O$ (90:8:2), a small but significant perturbation of the UV–vis spectrum was observed after addition of 8 equiv of $HP_2O_7^{3-}$, consisting of a hyperchromic effect of all bands in the spectrum. A good binding profile was obtained with a clear saturation at the end of the titration (see the Supporting Information). A Job plot indicates a 1:1 stoichiometry of the complex.

Perturbation of the emission of receptor **4** in the presence of the above-mentioned anions was also studied. Only addition of $HP_2O_7^{3-}$ anion induced any change in the fluorescence spectrum. Thus, the progressive addition of 32 equiv of this anion ($c = 1 \times 10^{-5}$ M, λ_{exc} = 350 nm) causes a decrease of the pyrene monomer band at λ_{emi} = 388 and 407 nm (Φ_F = 0.053) and an increase of the excimer band at λ_{emi} = 438 nm (Φ_F = 0.046), which is a broad and structureless red-shifted band (Figure 2). During the course of the titration an isoemissive

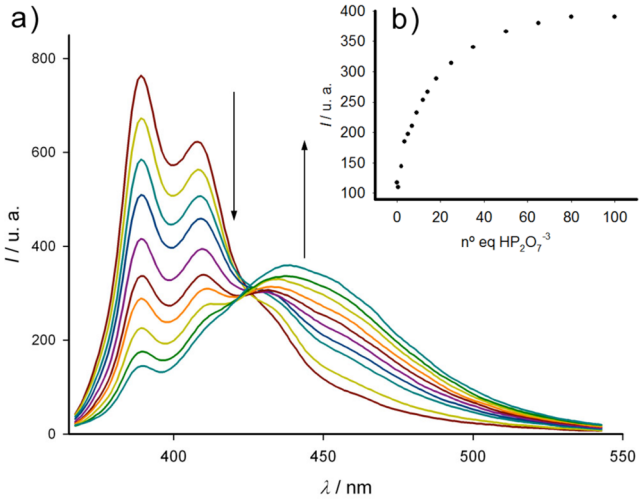

Figure 2. (a) Variation of the fluorescence spectrum of **4** ($c = 1 \times 10^{-5}$ M) in $CH_3CN/CH_2Cl_2/H_2O$ (90:8:2), λ_{exc} = 350 nm, upon addition of increasing amounts of $HP_2O_7^{3-}$ as a tetrabutylammonium salt. (b) Binding profile of the titration at λ = 450 nm.

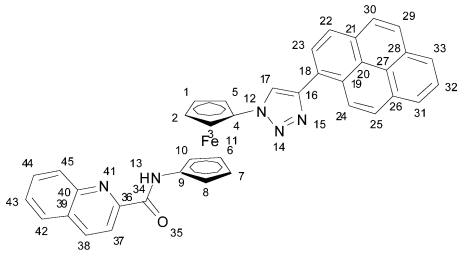

Figure 3. Atom numbering used in the assignation of NMR signals.

point at λ = 425 nm was conserved. This is indicative of the prevalence of the equilibrium established between the two species. This result demonstrates that receptor **4** behaves as a ratiometric fluorescent probe for $HP_2O_7^{3-}$ without the influence of $H_2PO_4^-$ or the rest of the anions tested. Moreover, the 1:1 stoichiometry formed in the UV–vis experiments together with the appearance of an excimer during the titration process strongly indicates that the formation of the final complex should take place with a 2:2 receptor:anion stoichiometry. The detection limit, calculated as 3 times the standard deviation of the background noise,[23] for $HP_2O_7^{3-}$ was found to be 1.4×10^{-5} M.

To obtain additional evidence of the recognition process taking place upon addition of $HP_2O_7^{3-}$ to the receptor **4**, we have also studied the changes that occur in the emission spectrum of the free receptor upon addition of Bu_4NOH under the same experimental conditions. In this case, a completely

dx.doi.org/10.1021/jo301570u | J. Org. Chem. 2012, 77, 10083–10092

different emission spectrum was obtained, the most characteristic features being that the monomer emission intensity does not decrease as the addition of the base is taking place and that the formation of a very broad band corresponding to the excimer emission is also observed (see the Supporting Information). This result, completely different from that observed by adding the $HP_2O_7^{3-}$ anion, constitutes more evidence that a hydrogen-bonded complex between the free ligand and this anion is formed, as was also concluded from the above-mentioned electrochemical studies.

^1H NMR experiments were carried out ($c = 5 \times 10^{-3}$ M) in CD_3CN/CD_2Cl_2 (4:1) to gain clarity about the coordination mode of $HP_2O_7^{3-}$. The peaks of the ^1H NMR spectrum were asigned by using $^1H-^1H$ COSY and HMQC bidimensional spectra (Figure 3) (see the Supporting Information). When growing amounts of $HP_2O_7^{3-}$ were added to the receptor solution, we observed the presence of two different tendencies. First, the amide proton that appears at 9.24 ppm readily vanishes with the addition of less than 1 equiv of the anion. Simultaneously, the triazole proton is deshielded, $\Delta\delta = 0.1$ ppm, while the other protons remain unaltered. Then from 0.5 to 4 equiv, the positions of all the signals in the spectrum do not experience any change, but further addition of $HP_2O_7^{3-}$ (up to 32 equiv) causes a more pronounced deshielding of the triazole proton that is simultaneously accompanied by displacement more downfield of the H-22 pyrene proton as well as by displacement of the quinoline protons to the upper field (Figure 4). The existence of two different processes during the ^1H NMR titration points to the formation of two different complexes.

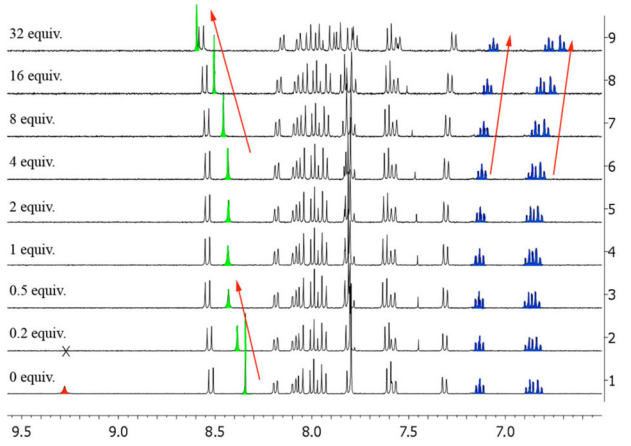

Figure 4. Variation of the ^1H NMR spectrum of **4** ($c = 5 \times 10^{-3}$ M in CD_3CN/CD_2Cl_2 (4:1)) upon addition of increasing amounts of $HP_2O_7^{3-}$.

When the complex of the receptor **4** formed with $HP_2O_7^{3-}$ was studied by ESI-MS, we observed the presence of a peak at m/z = 1041.5 that can be assigned to a 1:1 complex (m/z = 799) accompanied by a molecule of tetrabuthylammonium (m/z = 242).

Quantum chemical calculations (B3LYP-D/def2-SVP) provided valuable information regarding the possible binding modes of the $HP_2O_7^{3-}$ guest unit to receptor **4**. For the sake of saving computational time and resources, the simplified model **5** was used (Figure 5). In this model the 1-pyrenyl group was replaced by a phenyl substituent, yet featuring the essential framework for binding, except when it comes to excimer

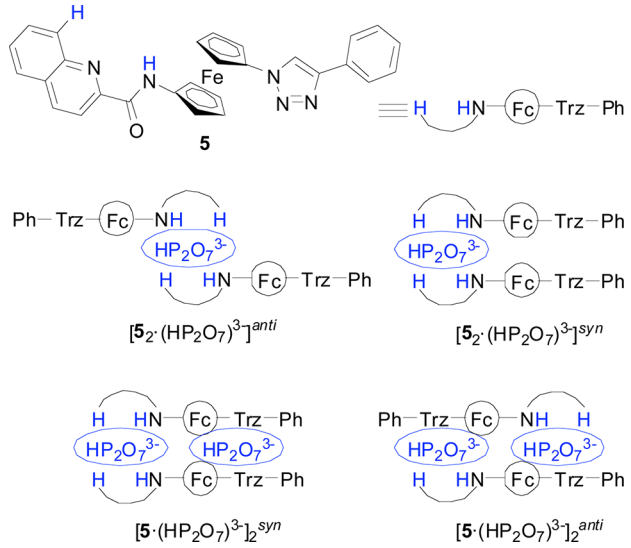

Figure 5. Model receptor **5** and possible stoichiometries and stereoisomers for complexes with $(HP_2O_7)^{3-}$.

formation. On the basis of the experimentally ascertained 1:1 ligand:pyrophosphate ratio and the fact that the simplest $[\mathbf{5}\cdot(HP_2O_7)^{3-}]$ molecularity could hardly explain the observed excimer emission that requires a parallel approach of two pyrene units, a 2:2 stoichiometry was assumed. Upon addition of the anion to the receptor, the first pyrophosphate unit, having remarkable basic character, would presumably bind two receptor **5** units, one at every phosphate site, through their most acidic quinaldoylamide moieties, leading to a $[\mathbf{5}_2\cdot(HP_2O_7)^{3-}]$ initial complex. An *anti* arrangement can be ruled out as it would locate the two aromatic units far apart, as well as the triazole rings that can behave as secondary anion binding sites.[6] The computed structure for the alternative $[\mathbf{5}_2\cdot(HP_2O_7)^{3-}]^{syn}$ complex (Figure S14, Supporting Information) displays a helix-shaped structure that also prevents excimer formation. The well-separated side arms in this $[\mathbf{5}_2\cdot(HP_2O_7)^{3-}]^{syn}$ complex can approach each other to allocate a second pyrophosphate unit between two pyrazole rings, giving rise to a minimum energy structure, $[\mathbf{5}\cdot(HP_2O_7)^{3-}]_2^{syn}$ (Figure S15, Supporting Information), that still maintains the terminal arene moieties far from a stacking distance. However, a secondary shallow well in the potential energy surface, featuring a lateral binding pattern of the second pyrophosphate anion with both triazole side arms, brings the terminal arene rings in close proximity (Figure S16, Supporting Information), thus accounting for the above-mentioned fluorescence emission structure.

The recognition properties of this receptor were also tested toward the above-mentioned set of metal cations, Li^+, Na^+ K^+, Ca^{2+}, Mg^{2+}, Ni^{2+}, Zn^{2+}, Cd^{2+}, Pb^{2+}, Cu^{2+}, and Hg^{2+}, in CH_3CN/CH_2Cl_2 (3:2). Only Pb^{2+} ($\Delta E_{1/2}$ = 75 mV, Figure 6) and Hg^{2+} ($\Delta E_{1/2}$ = 155 mV) induced changes with a moderate amount of the cation (10 equiv), whereas Ni^{2+} or Zn^{2+} caused perturbations with a large amount of the cation (>100 equiv). When these studies were carried out by UV–vis spectroscopy ($c = 2 \times 10^{-5}$ M) in CH_3CN/CH_2Cl_2 (3:2), the results obtained indicated that when up to 10 equiv of metal was added, only Pb^{2+} and Hg^{2+} induced an appreciable hyperchromic effect on the absorption spectrum of the free receptor. Job's plots obtained from these titration data suggest

dx.doi.org/10.1021/jo301570u | J. Org. Chem. 2012, 77, 10083–10092

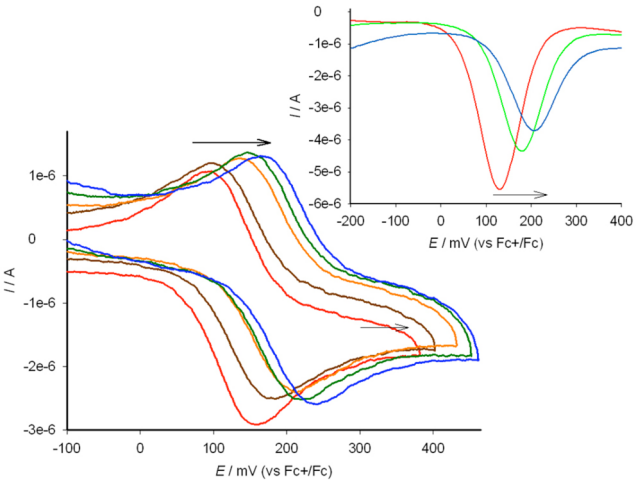

Figure 6. Variation of the redox potential of the ferrocene unit of **4** (c = 5 × 10^{-4} M) in CH_3CN/CH_2Cl_2 (3:2) upon addition of 0, 1, 3, 8, and 12 equiv of Pb^{2+}. Inset: Osteryoung square-wave voltammogram of **4** with 0, 6, and 12 equiv of Pb^{2+}.

the formation, in both cases, of complexes with a 1:1 stoichiometry (see the Supporting Information).

When fluorescence measurements were performed for cations in CH_3CN/CH_2Cl_2 (3:2) (c = 1 × 10^{-6} M, λ_{exc} = 350 nm), only Hg^{2+} caused variations in the emission properties of the receptor **4**. This change consists of a progressive decrease in the monomer emission intensity of about 85% (from Φ_F = 0.071 to Φ_F = 0.012) with the addition of 60 equiv of Hg^{2+} (Figure 7). The detection limit[23] for Hg^{2+}

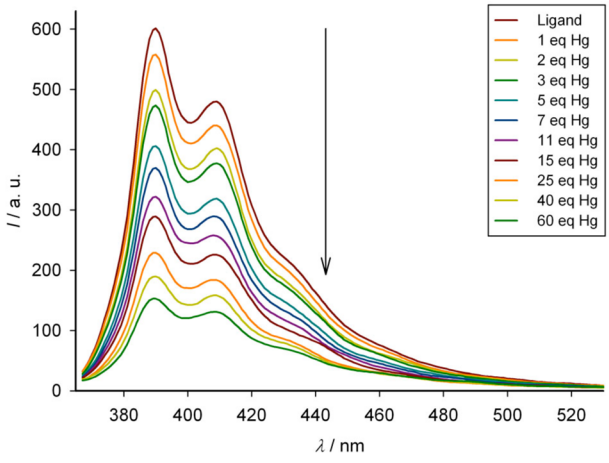

Figure 7. Variation of the emission spectrum of **4** (c = 1 × 10^{-6} M) in CH_3CN/CH_2Cl_2 (3:2), λ_{exc} = 350 nm, upon addition of increasing amounts of Hg^{2+} as a triflate salt.

was found to be 7.5 × 10^{-7} M. It is worth mentioning that while Pb^{2+} and Hg^{2+} induce significant changes in the oxidation potential and UV−vis spectrum of the free ligand, the emission spectrum is only modified upon addition of Hg^{2+} metal cations.

The binding modes taking place in the formation of the complexes between receptor **4** and the cations have been studied by ^{1}H NMR titrations. Due to the small solubility of the metal complexes formed, at the end of the titrations the intensities of the peaks decrease, especially in the case of Hg^{2+}, where the signals in the spectrum rapidly vanished with the addition of this cation. However, for Pb^{2+}, the formation of the complex could be successfully followed by this technique. Addition of an increasing amount of Pb^{2+} to a solution of **4** (c = 5 × 10^{-3} M) in CD_3CN/CD_2Cl_2 (4:1) caused a progressive downfield shifting of the amide proton (from δ = 9.28 ppm to δ = 9.58 ppm) after addition of 2 equiv of Pb^{2+}. Moreover, H_β and H_β' within the two monosubstituted cyclopentadienyl units present in the ferrocene moiety experienced a significant downfield shifting (from δ = 4.34 and 4.16 ppm to δ = 4.45 and 4.36 ppm, respectively). Simulteneously, the signals assigned to the pyrene unit suffer, in general, an upfield shifting and the quinoline protons a downfield shifting (Figure 10 and the Supporting Information). These ^{1}H NMR results suggest that the metal cations are simulteneously bound by the amide and triazole groups with a 1:1 stoichiometry.

All aforementioned results demonstrate that compound **4** binds $Hg^{2+}$and Pb^{2+} in a 1:1 fashion, as can be observed in the UV−vis, electrochemal, and ^{1}H NMR titrations, but only Hg^{2+} modifies the fluorescent emission of the pyrene unit. Therefore, this receptor **4** behaves as a selective on−off fluorescent sensor for Hg^{2+} with a low detection limit.

The association constants of **4** with $HP_2O_7^{3-}$ and Pb^{2+} were studied by isothermal titration calorimetry (ITC) (Figure 8). For the anion, the titration isotherm shows two different processes, the first one exothermic and the second endothermic, that occur with 2:1 and 1:1 stoichiometries (ligand:anion). Taking into account the experimental results found with the other techniques, we assume that the processes are in fact the formation of an initial 2:1 complex that evolves to the formation of a 2:2 stoichiometry complex. As can be seen in the ITC data, the complexation processes are mainly driven by entropy (ΔS_1 = 30.14 kcal/(mol·K) and ΔS_2 = 27.41 kcal/(mol·K)), although we observe that the first complexation step is also favored by enthalpy. Taking these data into account and the fact that we observe an evolution from a 2:1 to a 2:2 receptor:anion stoichiometry, we can assume that most of the conformational changes, which entail an enthalpic contribution, take place during the formation of the first complex. Therefore, the second complexation step should exclusively be favored by the release of solvent and other entropic effects. Such sequential exothermic and endothermic processes have already been described in the literature.[24] The global association constants found were $\beta_{2:1}$ = 1.0 × 10^8 M^{-2} and $K_{2:2}$ = 1.9 × 10^5 M^{-1}.

In the case of Pb^{2+}, the binding isotherm exhibits an exothermal process with a 1:1 stoichiometry and an association constant of $K_{1:1}$ = 4.9 × 10^3 M^{-1} (Figure 8). Binding constants for $HP_2O_7^{3-}$ and Pb^{2+} were also studied by UV−vis spectroscopy. In the case of Pb^{2+} a value of $K_{1:1}$ = 1.1 × 10^4 M^{-1}, similar to the ITC constant, was found. However, the $HP_2O_7^{3-}$ constant could not be accurately calculated due to its high magnitude, although it was of the same order as the ITC constants.

The formation of the metal complexes of **4** has also been studied by ESI-MS experiments, and the presence of the complexes is indicated by the presence of peaks that correspond to an m/z of the 1:1 complexes and also the peaks that correspond to half of this value, due to the 2+ charge of these complexes (see the Supporting Information).

Ion Pair Binding Studies. Moving one step further and taking into account the recognition capabilities of the receptor **4** for both anions and cations, we studied the binding of ion pairs in solution. For this reason, we followed by UV−vis spectroscopy, ^{1}H NMR spectroscopy, and fluorescence and

dx.doi.org/10.1021/jo301570u | J. Org. Chem. 2012, 77, 10083−10092

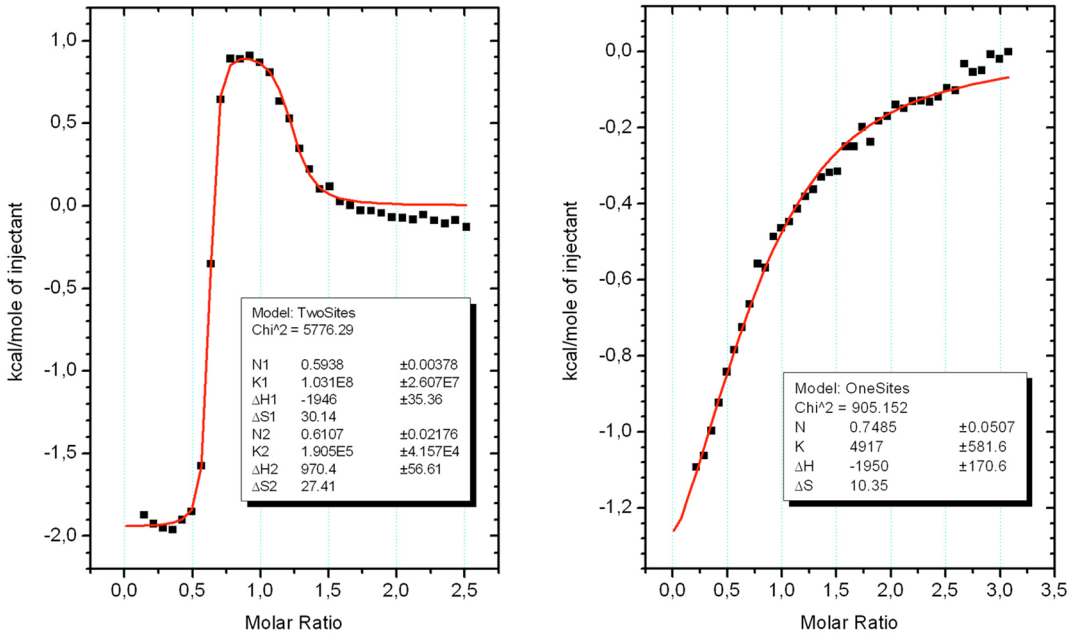

Figure 8. ITC titration plots of receptor **4** with $HP_2O_7^{3-}$ (left) and Pb^{2+} (right) in CH_3CN/CH_2Cl_2 (3:2). Normalized integration data of the evolved heat per injection in terms of kcal·mol^{-1} of injectant are plotted against the molar ratio (titrant:ligand).

electrochemical methods the influence of the addition to **4** of anions and cations simultaneously. In general, the addition of Ni^{2+}, Zn^{2+}, or Hg^{2+} to the previously formed complex with anions only causes the dissociation of the complex and further complexation with the excess of the metal added. The same behavior was found when the anions were added to the preformed cation complexes. However, the combination of Pb^{2+} and $HP_2O_7^{3-}$ induced a different response. One of the most important differences was found in UV–vis spectroscopy. Neither anion nor cation causes a remarkable change of the color when a few equivalents was added to a solution of **4**. However, when 1 equiv of Pb^{2+} and 1 equiv of $HP_2O_7^{3-}$ were added, a new red-shifted band appeared at λ = 600 nm which is responsible for the change of color from yellow to green (Figure 9). By contrast, when the same experiment was carried out by using 1 equiv of Hg^{2+}, the formation of the insoluble $Hg_3[HP_2O_7]_2$ salt was obtained, the free ligand remaining in the solution as was confirmed by spectroscopic methods.

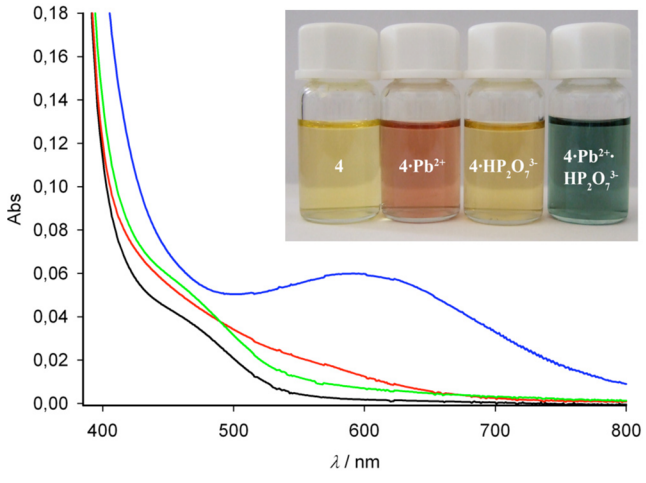

Figure 9. Changes in the UV–vis spectra of **4** (black) upon addition of 1 equiv of Pb^{2+} (red), 1 equiv of $HP_2O_7^{3-}$ (green), or a mixture of 1 equiv of Pb^{2+} and 1 equiv of $HP_2O_7^{3-}$ (blue). Inset: change of the color of the solution with the formation of the different complexes.

The formation of this ion pair was also monitored by ^{1}H NMR, and a new spectrum, different from those of the free receptor, the anion, or the cation complexes, was found with the addition of 1 equiv of Pb^{2+} and 1 equiv of $HP_2O_7^{3-}$. In the resulting new spectrum, the NH proton of the amide appeared slightly shielded with respect to that of the free ligand ($\Delta\delta$ = −0.21 ppm, while with anions this proton disappears and with cations is downfield shifted to δ = 9.65 ppm). On the other hand, the protons of triazole and H-22 of the pyrene unit were also deshielded, more than they were in the presence of the anions or cations alone (δ = 8.41 and 8.64 ppm, respectively), indicating the participation of both units (triazole and amide) in the binding of the ion pair complex. Moreover, the ferrocene protons are in an intermediate position compared to those of the anion or cation complexes alone. Particularly, deshielding of the H_α and H_α' protons was observed, while the H_β and H_β' protons were not disturbed. Another important difference is that a significant downfield shifting of the H-37 and H-38 protons of the quinoline ring is observed while the H-42 to H-45 protons are upfield shifted, different from the general behavior with cations or anions alone consisting of an upfield shifting of the signals. These results strongly suggest the formation of a different complex bearing Pb^{2+} and $HP_2O_7^{3-}$ (Figures 10 and 11).

When the titrations were followed by electrochemical techniques, addition of 3 equiv of Pb^{2+} and 3 equiv of $HP_2O_7^{3-}$ to the receptor **4** caused the appearance of a new oxidation peak at $E_{1/2}$ = 150 mV anodically shifted ($\Delta E_{1/2}$ = 30 mV) with respect to that of the free receptor **4** ($E_{1/2}$ = 120 mV) and different from the oxidation potentials of the complex [**4**·$HP_2O_7^{3-}$]$_2$ ($E_{1/2}$ = 10 mV) and the complex [**4**·Pb^{2+}] ($E_{1/2}$ = 205 mV) (Figure 12).

The emission propierties of the free receptor **4** underwent a strong perturbation when the formation of the ion pair complex

dx.doi.org/10.1021/jo301570u | J. Org. Chem. 2012, 77, 10083–10092

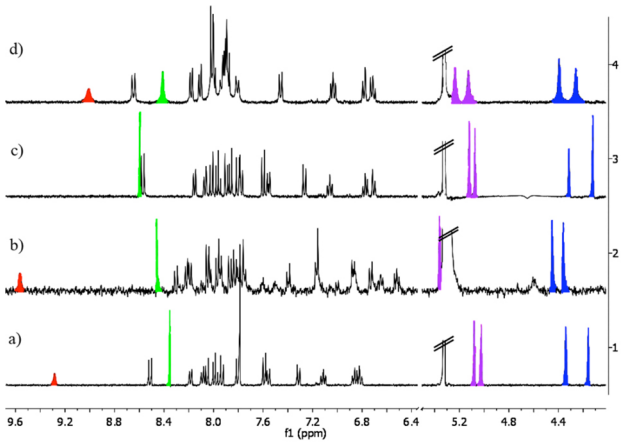

Figure 10. ^{1}H NMR spectra (c = 5 × 10^{-3} M in CD_3CN/CD_2Cl_2 (4:1)) of (a) the free receptor **4**, (b) the receptor and 1.5 equiv of Pb^{2+}, (c) the receptor and 16 equiv of $HP_2O_7^{3-}$, and (d) **4** with the addition of 1.5 equiv of Pb^{2+} and 2 equiv of $HP_2O_7^{3-}$.

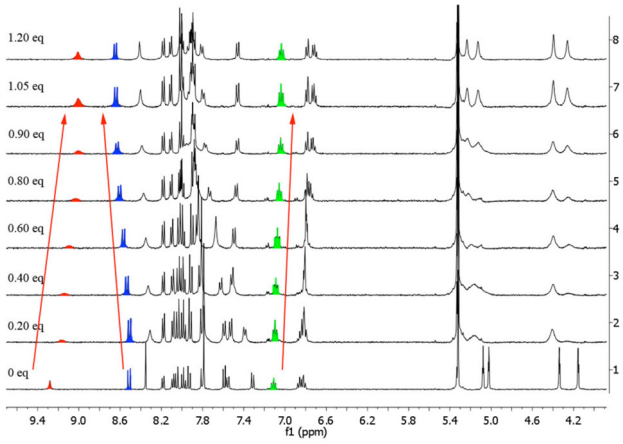

Figure 11. Variation of the ^{1}H NMR spectrum of **4** (c = 5 × 10^{-3} M) in CD_3CN/CD_2Cl_2 (4:1) upon simultaneous addition of increasing equimolecular amounts of $HP_2O_7^{3-}$ and Pb^{2+}.

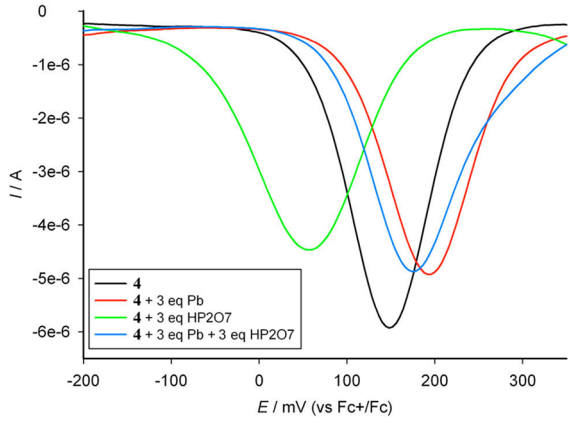

Figure 12. OSWV curves of the free receptor **4** (black) and the receptor with the addition of 3 equiv of Pb^{2+} (red), with 3 equiv of $HP_2O_7^{3-}$ (green), and with a mixture of both anion and cation (blue).

took place. When increasing amounts of Pb^{2+} were added to the preformed $[\mathbf{4}\cdot HP_2O_7^{3-}]_2$ complex, the excimer band decreased until disappearance and the monomer emission band increased until it reached half the intensity observed for the free receptor (Φ_F = 0.013). These results also support the formation of a structure different from the anion or cation complexes (Figure 13). Moreover, the preformed anion complex can be used as a

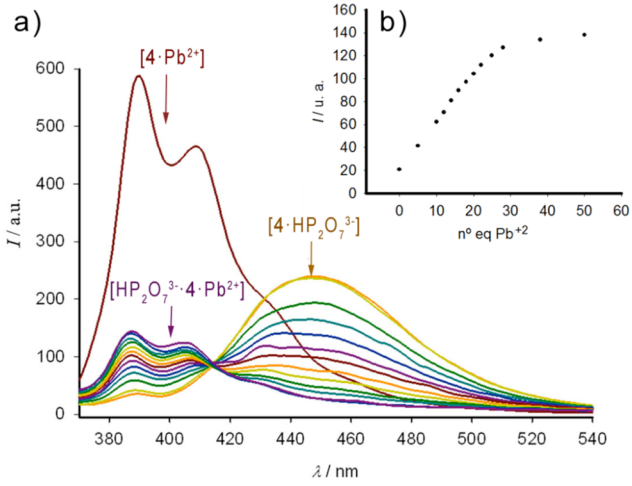

Figure 13. (a) Evolution of the emission spectrum of the complex $[\mathbf{4}\cdot HP_2O_7^{3-}]$ (c = 1 × 10^{-6} M) (yellow line) in CH_3CN/CH_2Cl_2 (3:2), λ_{exc} = 350 nm, upon addition of increasing amounts of Pb^{2+} as a triflate salt until formation of the ion pair $[HP_2O_7^{3-}\cdot\mathbf{4}\cdot Pb^{2+}]$ complex (magenta line). The brown line corresponds to the emission spectrum obtained upon addition of Pb^{2+} to the free ligand **4**. (b) Binding profile of the titration of $[\mathbf{4}\cdot HP_2O_7^{3-}]$ with Pb^{2+}, obtained at λ = 390 nm.

ratiometric sensor for Pb^{2+} cation, while in the absence of anion this cation does not change the emission properties of the receptor. The detection limit[23] for Pb^{2+} was found to be 8.2 × 10^{-6} M.

According to the DFT calculations, the minimum energy structure for the $[(HP_2O_7)\cdot\mathbf{4}\cdot Pb]^-$ ion pair complex, at the same level as the above-mentioned structures, involves deprotonation of the amide NH group in **4**. Nevertheless, this structure is not compatible with experimental observations, and a refinement of the structure using the higher level def2-TZVP basis set was required to end up with a non-deprotonated absolute minimum that seems to represent more likely the actual structure for the $[(HP_2O_7)\cdot\mathbf{4}\cdot Pb]^-$ ion pair complex (Figure 14). This results in the $(HP_2O_7)^{3-}$ anion

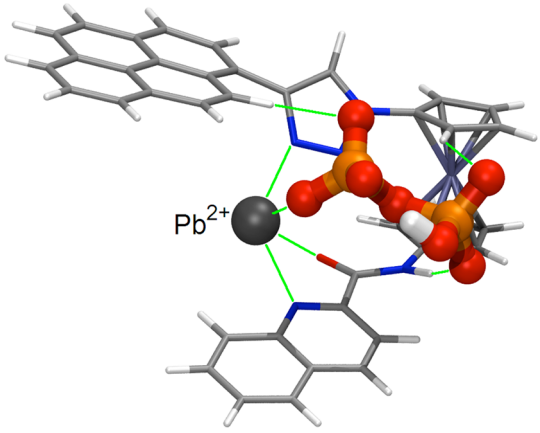

Figure 14. Computed ($COSMO_{MeCN}$/B3LYP-D/def2-TZVPecp) most stable geometry for the $[(HP_2O_7)\cdot\mathbf{4}\cdot Pb]^-$ complex. Key: Pb, gray; P, orange; O, red; N, blue; Fe, ice blue.

dx.doi.org/10.1021/jo301570u | J. Org. Chem. 2012, 77, 10083−10092

being strongly H-bonded to the amide NH group ($d_{O\cdots HN}$ = 1.669 Å) as well as to ferrocenyl ($d_{O\cdots H}$ = 2.409 and 2.440 Å) and pyrenyl ($d_{O\cdots H}$ = 2.328 Å) H atoms while occupying one of the coordinative positions around the metal cation (d_{O-Pb} = 2.192 Å). The receptor **4** wraps the metal cation through the triazole N3 atom (d_{N-Pb} = 2.562 Å), the markedly ionized amide O atom (d_{O-Pb} = 2.466 Å), and the quinoline N atom (d_{N-Pb} = 2.634 Å), together with a supplementary large contact to the pyrenyl C-10 atom (C-24 according to the overall numbering scheme in Figure 3) ($d_{C\cdots Pb}$ = 3.551 Å). Very likely, in acetonitrile solution one solvent molecule (at least) could be located at the coordination sphere around the large Pb^{2+} cation.

The different information obtained about the coordination of the different species indicates that $HP_2O_7^{3-}$ forms a 2:2 complex with the NH and CH protons of the amide and triazole units, forming hydrogen bonds with the anion. Moreover, the two pyrene units should be placed near enough to permit the formation of an excimer in solution. In the case of cations, a 1:1 stoichiometry was assumed, and the binding points are possibly one nitrogen atom of the triazole unit, the oxygen atom of the amide, and the nitrogen atom of the quinoline ring (see the Supporting Information). In the case of the ion pair complex, the experimental results suggest a 1:1:1 stoichiometry.

The association constant for the formation of the ion pair bound to **4** was calculated by ^{1}H NMR and emission spectroscopy instead of by ITC due to difficulties related to the solubility of the species formed. Values of $K_{1:1} = 1.58 \times 10^4$ M^{-1} by ^{1}H NMR and $K_{1:1} = 1.42 \times 10^4$ M^{-1} by fluorescence spectroscopy indicate that the stability of the bound ion pair is similar to that of the complex formed with Pb^{2+} and $HP_2O_7^{3-}$, which is in agreement with the experimental results.

CONCLUSIONS

The unsymmetrical 1,1′-disubstituted ferrocene receptor **4**, bearing a pyrenyl-substituted triazole ring linked at one cyclopentadienyl unit, formed via click-type chemistry, and an *N*-quinolyl-substituted amide at the other one, generated by an initial Staudinger reaction and subsequent acylation, has been prepared from the 1,1′-bisazidoferrocene. This receptor behaves as a true lab-on-a-molecule probe, and its sensing properties have been studied for different anions and metal cations. The receptor exhibits a reversible oxidation wave, and only $HP_2O_7^{3-}$ anion induced a remarkable cathodic shift of the oxidation peak ($\Delta E_{1/2}$ = −110 mV), whereas addition of Pb^{2+} ($\Delta E_{1/2}$ = 75 mV) and Hg^{2+} ($\Delta E_{1/2}$ = 155 mV) induced an anodic shift of the oxidation wave.

A small but significant perturbation of the UV−vis spectrum is observed after addition of $HP_2O_7^{3-}$, consisting of a hyperchromic effect of all bands in the spectrum; similar results are obtained when Pb^{2+} and Hg^{2+} are added. Addition of $HP_2O_7^{3-}$ anion induced changes in the fluorescence spectrum: a decrease of the pyrene monomer band and an increase of the excimer band. This result demonstrates that receptor **4** behaves as a selective ratiometric fluorescent probe for $HP_2O_7^{3-}$; likewise, only Hg^{2+} modifies the fluorescent emission of the pyrene unit. Therefore, receptor **4** also behaves as a selective on−off fluorescent sensor for Hg^{2+}. The most salient feature of receptor **4** is its capability to act as an electrooptical ion pair recognition receptor, because it is able to simultaneously recognize Pb^{2+} cations in the presence of a cobound $HP_2O_7^{3-}$ anion through variation of the oxidation potential of the ferrocene/ferrocenium redox couple, remarkable perturbation of the emission spectrum, and a noticeable red shift of the LE band of the absorption spectrum, which is responsible for the color change from yellow to green, which allows the detection of the ion pair complex formation. From these results receptor **4** can be considered as a true lab-on-a-molecule probe.

EXPERIMENTAL SECTION

General Experimental Methods. All reactions were carried out under N_2 and using solvents which were dried by routine procedures. Commercial starting materials (quinaldoyl chloride, ferrocene, *n*-butyllithium, and ethynylferrocene) were used without further purification. 1,1′-Bisazidoferrocene was prepared as described previously in the literature.[18] Melting points were determined on a hot-plate melting point apparatus and are uncorrected. ^{1}H and ^{13}C spectra were recorded on a 200, 300, or 400 MHz apparatus. The following abbreviations have been used for stating the multiplicity of the signals: s (singlet), d (doublet), t (triplet), st (pseudotriplet), m (multiplet), q (quaternary carbon). Chemical shifts refer to signals of tetramethylsilane in the case of ^{1}H and ^{13}C spectra. CV and OSWV techniques were performed with a conventional three-electrode configuration consisting of platinum working and auxiliary electrodes and a Ag/AgCl reference electrode. The experiments were carried out with a 5×10^{-4} M solution of sample in an adequate solvent containing 0.1 M $(n\text{-}C_4H_9)_4NPF_6$ ($(TBA)PF_6$) as the supporting electrolyte. All the potential values reported are relative to the ferrocene couple at room temperature. Deoxygenation of the solutions was achieved by bubbling nitrogen for at least 10 min, and the working electrode was cleaned after each run. The cyclic voltammograms were recorded with a scan rate increasing from 0.05 to 1.00 V s^{-1}, while the OSWV curves were recorded at a scan rate of 100 mV s^{-1} with a pulse height of 10 mV and a step time of 50 ms. Typically, receptor (5×10^{-4} M) was dissolved in the appropriate solvent (5 mL) and (TBA)HP (base electrolyte) (0.194 g) added. The guest under investigation was then added as a 2.5×10^{-2} M solution in the appropriate solvent using a microsyringe while the cyclic voltammetric properties of the solution were monitored. Fc was used as an external and/or internal reference both for potential calibration and for reversibility criteria. Under similar conditions, Fc has E = 0.39 V vs SCE and the anodic−cathodic peak separation is 67 mV. UV−vis and fluorescence spectra were obtained in the solvents and concentrations stated in the text and in the corresponding figure captions. Quantum yield values were measured with respect to anthracene as the standard ($\Phi = 0.27 \pm 0.01$)[25] using the equation $\Phi_x/\Phi_s = (S_x/S_s)\,[(1 - 10^{-A_s})/(1 - 10^{-A_x})](n_s^2/n_x^2)$, where x and s indicate the unknown and standard solutions, respectively, F is the quantum yield, S is the area under the emission curve, A is the absorbance at the excitation wavelength, and n is the refractive index.

X-ray data for compound 4: $C_{38}H_{25}FeN_5O$, M_r = 623.48, 0.27 × 0.21 × 0.18 mm size, orthorhombic, $P2_12_12_1$, a = 9.002(3) Å, b = 13.0829(3) Å, c = 21.7792(6) Å, V = 2763.93(13) Å^3, Z = 4, ρ_{calcd} = 1.498 g cm^{-3}, μ = 0.589, Mo Kα, λ = 0.71073 Å, T = 120(2) K, $2\theta_{max}$ = 64.72°, 27718/9167 reflections collected/independent (R_{int} = 0.0416), direct primary solution and refinement on F^2 (SHELXS-97 and SHELXL-97, G. M. Sheldrick, University of Göttingen, 1997), 410 parameters, hydrogen atoms refined as free for N−H, others *riding*, R1[$I > 2\sigma(I)$] = 0.0386, wR2(all data) = 0.0850, $\Delta\rho_{max}$ = 0.37 e Å^{-3}.

Computational Details. All calculations were carried out with the ORCA electronic structure program package,[26] with all structures being optimized in redundant internal coordinates at the density functional theory (DFT) level using the B3LYP[27] functional together with the new efficient RIJCOSX algorithm[28] and the def2-SVP[29] basis set. Only the structure for the ion pair $[(HP_2O_7)\cdot\mathbf{4}\cdot Pb]^-$ complex was further refined with the def2-TZVP[30] basis set. For Pb the [SD(60,MDF)] effective core potential was employed.[31] A damped semiempirical correction accounting for the major part of the contribution of dispersion forces to the energy was included[32] and denoted with suffix "-D" after the name of the functional (B3LYP-D). Solvent effects (MeCN) were taken into account via the COSMO solvation model.[33]

dx.doi.org/10.1021/jo301570u | J. Org. Chem. 2012, 77, 10083−10092

Synthesis of 1-[4-(1-Pyrenyl)-1,2,3-triazol-1-yl)]-1′-azidoferrocene, 1. To a solution of 1,1′-bisazidoferrocene[18] (0.250 g, 0.93 mmol) and 1-ethynylpyrene (0.221 g, 0.97 mmol) in THF (80 mL) was added a solution $CuSO_4$ (0.075 g, 0.30 mmol) in water (15 mL). Then a freshly prepared solution of sodium ascorbate (0.249 g, 1.25 mmol) in water (15 mL) was added dropwise, and the reaction mixture was stirred at room temperature for 12 h. After removal of THF under vacuum, EtOAc (0.1 mL) and CH_2Cl_2 (4.9 mL) were added, and the resulting solution was chromatographed on a silica gel column using CH_2Cl_2/EtOAc (98:2) as the eluent (R_f = 0.5). Once the solvent was removed under vacuum, a brown solid was obtained which was identified as the desired product (0.185 g, 40%) and used without further purification. Mp: 95 °C ded. ^{1}H NMR (400 MHz, CD_2Cl_2): δ 8.75 (d, J = 12 Hz, 1H), 8.29 (d, J = 8 Hz, 1H,), 8.23 (d, J = 8 Hz, 1H), 8.21 (s, 1H), 8.19 (s, 2H), 8.15 (d, J = 12 Hz, 1H), 8.09 (d, J = 4 Hz, 2H), 8.02 (t, J = 8 Hz, 1H), 5.08 (st, 2H), 4.42 (st, 2H), 4.35 (st, 2H), 4.18 (st, 2H). ^{13}C{^{1}H} NMR (101 MHz, $CDCl_3$): δ 148.6, 132.3, 132.2, 131.8, 129.6, 129.2, 128.8, 128.3, 128.1 127.0, 126.3, 126.1, 125.9, 125.8, 125.7, 125.6, 123.0, 101.7, 95.6, 68.7, 68.4, 63.9, 63.1. FT-IR (CH_2Cl_2): ν = 2109 cm^{-1} (N_3). MS (ESI): m/z 495 (68, M^+ + 1). Anal. Calcd for $C_{28}H_{18}FeN_6$: C, 68.03; H, 3.67; N, 17.00. Found: C, 68.28; H, 3.95; N, 16.69.

Synthesis of 1-[4-(1-Pyrenyl)-1,2,3-triazol-1-yl]-1′-aminoferrocene, 3. To a solution of compound **1** (0.05 g, 0.10 mmol) in anhydrous THF (40 mL) was added trimethylphosphine (0.5 mL, 0, 5 mmol) under a N_2 atmosphere. The mixture was stirred for 30 min at room temperature, and then water (1 mL) was added. The solution was then stirred for 12 h at room temperature, and later, the THF was removed under vacuum. The resulting residue was extracted with a mixture of CH_2Cl_2 (50 mL) and water (20 mL). The organic phase was dried over anhydrous $MgSO_4$ and the solvent removed, yielding a brown solid identified as the desired product (0.100 g, 64%) which was used without further purification. Mp: 208 °C ded. ^{1}H NMR (400 MHz, CD_2Cl_2): δ 8.75 (d, J = 12 Hz, 1H), 8.28 (d, J = 8 Hz, 1H), 8.23 (d, J = 8 Hz, 1H), 8.19 (s, 1H), 8.16 (s, 2H), 8.14 (d, J = 12 Hz, 1H), 8.10 (d, J = 4 Hz, 2H), 8.02 (t, J = 8 Hz, 1H), 4.87 (st, 2H), 4.27 (st, 2H), 4.05 (st, 2H), 3.97 (st, 2H); ^{13}C{^{1}H} NMR (101 MHz; $CDCl_3$): δ 147.3, 131.4, 130.8, 128.8, 128.6, 128.3, 127.9, 127.3, 127.0, 126.1, 125.4, 125.1, 125.0, 124.9, 124.8, 124.7, 122.4, 107.9, 93.7, 67.2, 65.2, 63.1, 59.9, FT-IR (CH_2Cl_2): ν = 3450, 3355 cm^{-1} (NH_2). MS (ESI): m/z 469 (100, M^+ + 1). Anal. Calcd for $C_{28}H_{20}FeN_4$: C, 71.81; H, 4.30; N, 11.96. Found: C, 72.02; H, 4.46; N, 11.69.

Synthesis of 1-[4-(1-Pyrenyl)-1,2,3-triazol-1-yl)]-1′-(quinaldoylamino)ferrocene, 4. To a solution of **3** (0.05 g, 0.11 mmol) in anhydrous THF (20 mL) were added 1-quinaldoyl chloride (0.021 g, 0.11 mmol) and triethylamine (0.2 mL) under a nitrogen atmosphere. The reaction mixture was stirred at room temperature for 6 h, and then the solvent was removed under reduced pressure, giving rise to a residue which was chromatographed in a silica gel column using EtOAc/CH_2Cl_2 (1:9) as the eluent (R_f = 0.67). The orange solid obtained was crystallized from CH_2Cl_2/diethyl ether (1:1) (57 mg, 86%). Mp: 208 °C dec. ^{1}H NMR (400 MHz; CD_2Cl_2): δ 9.24 (s, 1H, H-13), 8.57 (d, J = 9.2 Hz, 1H, H-22), 8.24 (d, J = 8.8 Hz, 1H, H-25), 8.23 (s, 1H, H-17), 8.12 (m, 2H, H-31 and H-33), 8.05 (t, J = 7.6 Hz, 1H, H-32), 8.03 (d, J = 8.8 Hz, 1H, H-24), 7.88 (br s, 2H, H-29 and H-30), 7.84 (d, J = 9.2 Hz, 1H, H-23), 7.78 (dd, J = 8.4, J = 0.8 Hz, 1H, H-45), 7.69 (d, J = 8.4 Hz, 1H, H-37), 7.33 (ddd, J = 8.4 Hz, J = 6.8 Hz, J = 0.8 Hz, 1H, H-44), 7.27 (d, J = 8.4 Hz, 1H, H-38), 7.02 (ddd, J = 7.2 Hz, J = 6.8 Hz, J = 0.8 Hz, 1H, H-43) 6.89 (dd, J = 7.2 Hz, J = 0.8 Hz, 1H, H-42), 5.13 (st, 2H, Fc), 5.07 (st, 2H, Fc), 4.42 (st, 2H, Fc), 4.24 (st, 2H, Fc). ^{13}C{^{1}H} NMR (101 MHz; CD_2Cl_2): δ 163.0 (q, CO), 148.7 (q), 147.5 (q), 146.2 (q), 137.3 (C-38), 131.8 (q), 131.3 (q), 131.3 (q), 130.1 (C-44), 129.3 (C-45), 129.0 (q), 128.1 (C-23), 128(C-31 or C-33), 127.7 (C-24), 127.7 (C-43), 127.3(C-42), 126. (C-29 or C-30), 126.4 (C-32), 125.6 (C-25), 125.5 (C-31 or C-33), 125.4 (C-22), 125.2 (C-29 or C-30), 125 (q), 124.9 (q), 122.6 (C-17), 118 (C-37), 97.1 (q, Fc), 95.2 (q, Fc), 67.7 (CH, Fc), 66.6 (CH, Fc), 63.0 (CH, Fc), 62.7 (CH, Fc). FT-IR (CH_2Cl_2): ν 3354 (NH), 1680 (CO) cm^{-1}. MS (ESI): m/z 624 (100, M^+ + 1). Anal. Calcd for $C_{38}H_{25}FeN_5O$: C, 73.20; H, 4.04; N, 11.23. Found: C, 73.39; H, 4.21; N, 11.13.

■ ASSOCIATED CONTENT

Ⓢ Supporting Information

Crystallographic information file (CIF) for compound **4** and additional NMR, electrochemical, UV−vis, ESI-MS, and DFT data. This material is available free of charge via the Internet at http://pubs.acs.org.

■ AUTHOR INFORMATION

Corresponding Author

*Fax: +34 868 884 149. Phone: +34 868 887 496. E-mail: pmolina@um.es; atarraga@um.es; franoton@um.es.

Notes

The authors declare no competing financial interest.

■ ACKNOWLEDGMENTS

We gratefully acknowledge financial support from MICINN-Spain, Project CTQ 2011/27175, and Fundación Séneca (Agencia de Ciencia y Tecnología de la Región de Murcia), Project 04509/GERM/06 (Programa de Ayudas a Grupos de Excelencia de la Región de Murcia, Plan Regional de Ciencia y Tecnología 2007/2010).

■ REFERENCES

(1) (a) Kirkovits, G. J.; Shriver, J. A.; Gale, P. A.; Sessler, J. L. *J. Inclusion Phenom. Macrocyclic Chem.* **2001**, *41*, 69−75. (b) Smith, B. D. In *Macrocyclic Chemistry: Current Trends and Future Perspectives*; Gloe, K., Ed.; Springer: Dordrecht, The Netherlands, 2005. (c) Zhu, K.; Zhang, M.; Wang, Z.; Li, N.; Li, S.; Huang, F. *New J. Chem.* **2008**, *32*, 1827−1830. (d) Zhu, K.; Li, S.; Wang, F.; Huang, F. *J. Org. Chem.* **2009**, *74*, 1322−1328. (e) Zhu, K.; Wu, L.; Yan, X.; Zheng, B.; Zhang, M.; Huang, F. *Chem.—Eur. J.* **2010**, *16*, 6088−6098. (f) Kim, S. K.; Sessler, J. L. *Chem. Soc. Rev.* **2010**, *39*, 3784−3809. (g) McConnell, A. J.; Beer, P. D. *Angew. Chem., Int. Ed.* **2012**, *51*, 5052−5061.

(2) (a) Lin, T. C.; Lai, C. C.; Chiu, S. H. *Org. Lett.* **2009**, *11*, 613−616. (b) Barrell, M. J.; Leigh, D. A.; Lusby, P. J.; Slawin, A. M. Z. *Angew. Chem., Int. Ed.* **2008**, *47*, 8036−8039. (c) Nielsen, K. A.; Sarova, G. H.; Martin-Gomis, L.; Fernandez-Lazaro, F.; Stein, P. C.; Sanguinet, L.; Levillain, E.; Sessler, J. L.; Guldi, D. M.; Sastre-Santos, A.; Jeppesen, J. O. *J. Am. Chem. Soc.* **2008**, *130*, 460−462. (d) Leontiev, A. V.; Jemmett, C. A.; Beer, P. D. *Chem.—Eur. J.* **2011**, *17*, 816−825.

(3) Blondeau, P.; Segura, M.; Pérez-Fernández, R.; de Mendoza, J. *Chem. Soc. Rev.* **2007**, *36*, 198−210.

(4) (a) Othman, A. M.; El-Houseini, M. E.; El-Sofy, M. S.; Aboul-Enein, H. Y. *Anal. Bioanal. Chem.* **2011**, *400*, 787−795. (b) Niikura, K.; Anslyn, E. V. *J. Org. Chem.* **2003**, *68*, 10156−10157.

(5) Ren, C.; Maurizot, V.; Zhao, H.; Shen, J.; Zhou, F.; Ong, W. Q.; Du, Z.; Zhang, K.; Su, H.; Zeng, H. *J. Am. Chem. Soc.* **2011**, *133*, 13930−13933.

(6) Ganesh, V.; Sudhir, V. S.; Kundu, T.; Chandrasekaran, S. *Chem.—Asian J.* **2011**, *6*, 2670−2694.

(7) (a) Bronisz, R. *Inorg. Chem.* **2005**, *44*, 4463−4465. (b) Li, Y.; Huffman, J. C.; Flood, A. H. *Chem. Commun.* **2007**, *26*, 2692−2694. (c) Chan, T. R.; Hilgraf, R.; Sharpless, K. B.; Fokin, V. V. *Org. Lett.* **2004**, *6*, 2853−2855. (d) Chang, K.-C.; Su, I.-H.; Senthilvelan, A.; Chung, W.-S. *Org. Lett.* **2007**, *9*, 3363−3366. (e) David, O.; Maisonneuve, S.; Xie, J. *Tetrahedron Lett.* **2007**, *48*, 6527. (f) Chang, K.-C.; Su, I.-H.; Lee, G.-H.; Chung, W.-S. *Tetrahedron Lett.* **2007**, *48*, 7274−7278. (g) Ornelas, C.; Aranzaes, J. R.; Salmon, L.; Astruc, D. *Chem.—Eur. J.* **2008**, *14*, 50−64. (h) Ornelas, C.; Salmon, L.; Aranzaes, J. R.; Astruc, D. *Chem. Commun.* **2007**, 4946−4948. (i) Huang, S.; Clark, R. J.; Zhu, L. *Org. Lett.* **2007**, *9*, 4999−5002. (j) David, O.; Maisonneuve, S.; Xie. *Tetrahedon Lett.* **2007**, *48*, 6527−6530. (k) Park, S. Y.; Yoon, J. H.; Hong., C. S.; Souane, R.; Kim, J. S.;

Mattews, S. E.; Vicens, J. *J. Org. Chem.* **2008**, *73*, 8212−8218. (l) Hung, H.-C.; Cheng, C.-W.; Ho, I.-T.; Cheng, W.-S. *Tetrahedron Lett.* **2009**, *50*, 302−305. (m) Suijkerbuijk, B. M. J. M.; Aerts, B. N.; Dijkstra, H. P.; Lutz, M.; Spek, A. L.; van Koten, G; Klein Gebbink, R. J. M. *Dalton Trans.* **2007**, 1273−1276. (n) Badèche, S.; Daran, J.-C.; Ruiz, J.; Astruc, D. *Inorg. Chem.* **2008**, *47*, 4903−4908. (o) Crowley, J. D.; Bandeen, P. H.; Hanton, L. R. *Polyhedron* **2010**, *29*, 70−83. (p) Kilpin, K. J.; Crowley, J. D. *Polyhedron* **2010**, *29*, 3111−3117.

(8) (a) Kumar, A.; Pandey, P. S. *Org. Lett.* **2008**, *10*, 165−168. (b) Haridas, V.; Lal, K.; Sharma, Y. K.; Upreti, S. *Org. Lett.* **2008**, *10*, 1645−1647. (c) Horne, W. S.; Yadav, M. K.; Scout, C. D.; Ghadiri, M. R. *J. Am. Chem. Soc.* **2004**, *126*, 15366−15367. (d) Li., Y.; Flood, A. H. *Angew. Chem., Int. Ed.* **2008**, *47*, 2649−2652. (e) Juwarker, H.; Lenhardt, J. M.; Pham, D. M.; Craig, S. L. *Angew. Chem., Int. Ed.* **2008**, *47*, 3740−3743. (f) Meudtner, R. M.; Hecht, S. *Angew. Chem., Int. Ed.* **2008**, *47*, 4926−4930. (g) Ornelas, C.; Aranzaes, J. R.; Cloutet, E.; Alves, S.; Astruc, D. *Angew. Chem., Int. Ed.* **2007**, *46*, 872−877. (h) Hua, Y.; Flood, A. H. *Chem. Soc. Rev.* **2010**, *39*, 1262−1271. (i) Romero, T.; Caballero, A.; Tárraga, A.; Molina, P *Org. Lett.* **2009**, *11*, 3466−3469. (j) Romero, T.; Orenes, R. A.; Espinosa, A.; Tárraga, A.; Molina, P. *Inorg. Chem.* **2011**, *50*, 8214−8224. (k) Otón, F.; González, M. C.; Espinosa, A.; Tárraga, A.; Molina, P. *Organometallics* **2012**, *31*, 2085−2096. (l) Yu, G.; Zhang, Z.; Han, C.; Xue, M.; Zhou, Q.; Huang, F. *Chem. Commun.* **2012**, *48*, 2958−2960.

(9) (a) Chang, K.-C; Su, V.; Wang, Y.-Y.; Chung, W.-S. *Eur. J. Org. Chem.* **2010**, 4700−4704. (b) Ni, X.-l.; Zeng, X.; Redshaw, C.; Yamato, T. *J. Org. Chem.* **2011**, *76*, 5696−5702. (c) Picot, S. C.; Mullaney, B. R.; Beer, P. D. *Chem.—Eur. J.* **2012**, *18*, 6230−6237.

(10) (a) Alfonso, M.; Tárraga, A.; Molina, P. *J. Org. Chem.* **2011**, *76*, 939−947. (b) Alfonso, M.; Espinosa, A.; Tárraga, A.; Molina, P. *Org. Lett.* **2011**, *13*, 2078−2081. (c) Alfonso, M; Espinosa, A.; Tárraga, A.; Molina, P. *Chem. Commun.* **2012**, *48*, 6848−6850.

(11) An unsymmetrically 1,1′-disubstituted ferrocene-based ditopic receptor containing a urea and a benzo crown ether shows remarkable color change in the presence of fluoride anion but in the absence of potassium cation: Miyaji, H.; Collinson, S. R.; Prokes, I.; Tucker, J. H. R. *Chem. Commun.* **2003**, 64−65.

(12) (a) Seyferth, D.; Withers, H. P., Jr. *Organometallics* **1982**, *1*, 1275−1282. (b) Wright, M. E. *Organometallics* **1990**, *9*, 853−856. (c) Lai, L.-L.; Dong, T.-Y. *J. Chem. Soc., Chem. Commum.* **1994**, 2347−2348. (d) Iftime, G.; Moreau-Bossuet, C.; Manoury, E.; Balavoine, G. G. A. *J. Chem. Soc., Chem. Commun.* **1996**, 527−528. (e) Dong, T.-Y.; Lai, L.-L. *J. Organomet. Chem.* **1996**, *509*, 131−134. (f) Grossel, M. C.; Hamilton, D. G.; Vine, T. A. *Tetrahedron Lett.* **1997**, *38*, 4639−4642. (g) Rodríguez, J. G.; Pleite, S. *J. Organomet. Chem.* **2001**, *637*−*639*, 230−239. (h) Chiffre, J.; Averseng, F.; Balavoine, G. G. A.; Daran, J. C.; Iftime, G.; Lacroix, P. G.; Manoury, E.; Nakatani, K. *Eur. J. Inorg. Chem.* **2001**, 2221−2226. (i) Yu, C. J.; Wan, Y.; Yowanto, H.; Li, J.; Tao, C.; James, M. D.; Tan, C. L.; Blackburn, G. F.; Meade, T. J. *J. Am. Chem. Soc.* **2001**, *123*, 11155−11161. (j) Song, H.; Kerman, K.; Kraatz, H. B. *Chem. Commun.* **2008**, 502−504. (k) Moriuchi, T.; Nomoto, A.; Yoshida, K.; Ogawa, A.; Hirao, T. *J. Am. Chem. Soc.* **2001**, *123*, 68−75.

(13) (a) Butler, I. R.; Quayle, S. C. *J. Organomet. Chem.* **1998**, *552*, 63−68. (b) Okamura, T.; Sakauye, K.; Ueyama, N.; Nakamura, A. *Inorg. Chem.* **1998**, *37*, 6731−6736. (c) Argyropoulos, N.; Coutouli-Argyropoulo, E. *J. Organomet. Chem.* **2002**, *654*, 117−122. (d) Coutouli-Argyropoulo, E.; Sideris, C.; Kokkinidis, G. *J. Organomet. Chem.* **2006**, *691*, 3909−3918. (e) Bertina, P. A.; Maedeb, T. J. *Tetrahedron Lett.* **2009**, *50*, 5409−5412.

(14) (a) Molina, P.; Tárraga, A.; Caballero, A. *Eur. J. Inorg. Chem.* **2008**, 3401−3417. (b) Molina, P.; Tárraga, A.; Alfonso, M. *Eur. J. Org. Chem.* **2011**, 4505−4518. (c) Bayly, S. R.; Beer, P. D.; Chen, G. Z. *Ferrocene* **2008**, 281−318.

(15) Winnick, F. M. *Chem. Rev.* **1993**, *93*, 587−614.

(16) (a) Gale, P. A. *Coord. Chem. Rev.* **2000**, *199*, 181−233. (b) Bao, X.; Zhou, Y. *Sens. Actuators, B* **2010**, *147*, 434−441. (c) Chmielewski, M. J.; Jurczak, J. *Chem.—Eur. J.* **2005**, *11*, 6080−6094. (d) Kondo, S.-I.; Hiraoka, Y.; Kurumatani, N.; Yano, Y. *Chem. Commun.* **2005**, 1720−1722. (e) Kang, J.; Jo, J. H.; In, S. *Tetrahedron Lett.* **2004**, *45*, 5225−5228. (f) Chmielewsli, M.; Jurczak, J. *Tetrahedron Lett.* **2004**, *45*, 6007−6010. (g) Chmielewski, M.; Kurczak, J. *Tetrahedron Lett.* **2005**, *46*, 3085−3088. (h) Kang, S. O.; Linares, J. M.; Powell, D.; VanderVelde, D.; Bowman-James, K. *J. Am. Chem. Soc.* **2003**, *125*, 10152−10153.

(17) Huang, W.; Zhu, H.-B.; Gou, S.-H. *Coord. Chem. Rev.* **2006**, *250*, 414−423.

(18) (a) Tárraga, A.; Otón, F.; Espinosa, A.; Velasco, M. D.; Molina, P.; Evans, D. J. *Chem. Commun.* **2004**, 458−459. (b) Otón, F.; Tárraga, A.; Molina, P. *Org. Lett.* **2006**, *8*, 2107−2110. (c) Otón, F.; Espinosa, A.; Tárraga, A.; Ramirez de Arellano, C.; Molina, P. *Chem.—Eur. J.* **2007**, *13*, 5742−5752.

(19) (a) Rostovtsev, V.; Green, L. G.; Kokin, V. V.; Sharpless, K. B. *Angew. Chem., Int. Ed.* **2002**, *41*, 2596−2599. (b) Tornoe, C. V.; Christensen, C.; Medal, M. *J. Org. Chem.* **2002**, *67*, 3057−3064.

(20) Caballero, A.; Lloveras, V.; Curiel, D.; Tárraga, A.; Espinosa, A.; García, R.; Vidal-Gancedo, J.; Rovira, C.; Wurst, K.; Molina, P.; Veciana, J. *Inorg. Chem.* **2007**, *46*, 825−838.

(21) Amendola, V.; Esteban-Gomez, D.; Fabrizzi, L.; Licchelli, M. *Acc. Chem. Res.* **2006**, *39*, 343−353.

(22) Zapata, F.; Caballero, A.; Espinosa, A.; Tárraga, A.; Molina, P. *J. Org. Chem.* **2008**, *73*, 4034−4044.

(23) Shortreed, M; Kopelman, R; Kuhn, M; Hoyland, B *Anal. Chem.* **1996**, *68*, 1414−1418.

(24) Linton., B. R.; Goodman, M. S.; Fan, E.; van Arman, S. A.; Hamilton, A. D. *J. Org. Chem.* **2001**, *66*, 7313−7319.

(25) Dawson, W. R.; Windsor, M. W. *J. Phys. Chem.* **1968**, *72*, 3251−3260.

(26) ORCA—an ab initio, DFT and semiempirical SCF-MO package, version 2.9.0, written by F. Neese, Max Planck Institute for Bioinorganic Chemistry, D-45470 Mülheim/Ruhr, Germany. 2012. http://www.mpibac.mpg.de/bac/logins/neese/description.php, accessed on June 2, 2012.

(27) (a) Becke, A. D. *J. Chem. Phys.* **1993**, *98*, 5648−5652. (b) Lee, C. T.; Yang, W. T.; Parr, R. G. *Phys. Rev. B* **1988**, *37*, 785−789.

(28) Neese, F.; Wennmohs, F.; Hansen, A.; Becker, U. *Chem. Phys.* **2009**, *356*, 98−109.

(29) Schaefer, A.; Horn, H.; Ahlrichs, R. *J. Chem. Phys.* **1992**, *97*, 2571−2577.

(30) Weigend, F.; Ahlrichs, R. *Phys. Chem. Chem. Phys.* **2005**, *7*, 3297−3305.

(31) Metz, B.; Stoll, H.; Dolg, M. *J. Chem. Phys.* **2000**, *113*, 2563−2569. ECP parameters for Pb [SD(60,MDF)] have been obtained from the pseudopotential library of the Stuttgart/Cologne group at http://www.theochem.uni-stuttgart.de/pseudopotentials/, accessed on June 2, 2012.

(32) (a) Grimme, S. *J. Comput. Chem.* **2004**, *25*, 1463−1476. (b) Grimme, S. *J. Comput. Chem.* **2006**, *27*, 1787−1799.

(33) (a) Klamt, A.; Schüürmann, G. *J. Chem. Soc., Perkin Trans. 2* **1993**, *220*, 799−805. (b) Klamt, A. *J. Phys. Chem.* **1995**, *99*, 2224−2235.